Structure of chlorine on Ag(111): Evidence of the (3×3) reconstruction

B. V. Andryushechkin,[1,*] V. V. Cherkez,[1,2] E. V. Gladchenko,[1,3] G. M. Zhidomirov,[1] B. Kierren,[2] Y. Fagot-Revurat,[2] D. Malterre,[2] and K. N. Eltsov[1,3]

[1]*International Joint Laboratory IMTAS, A.M. Prokhorov General Physics Institute, Russian Academy of Sciences, Vavilov Str. 38, 119991 Moscow, Russia*

[2]*International Joint Laboratory IMTAS, Institut Jean Lamour, UMR CNRS 7198, équipe 102, Departement Physique de la Matière et des Matériaux, Université H. Poincaré–Nancy, BP 239, 54506 Vandoeuvre les Nancy, France*

[3]*Moscow Institute of Physics and Technology, Institutskii per. 9, 141700 Dolgoprudny, Moscow Region, Russia*

(Received 6 May 2010; published 25 May 2010)

The structure of the chlorine induced reconstruction of Ag(111) has been studied by a combination of low-temperature scanning tunneling microscopy (STM), low-energy electron diffraction (LEED), and density-functional theory (DFT). We demonstrate that previously observed mysterious LEED pattern arises as a result of diffraction from a system of small (15–30 Å) triangular antiphase domains with a new (3×3) superstructure. In our model supported by DFT calculations, within a (3×3) unit cell the upper silver layer reconstructs forming a couple of three-atom triangles placed in fcc and hcp sites of the substrate. Chlorine atoms occupy fourfold hollow sites between these triangles. The corner holes, which look like depressions in the STM images, are also occupied by chlorine atoms.

DOI: 10.1103/PhysRevB.81.205434 PACS number(s): 68.43.Fg, 68.43.Bc, 68.47.Fg, 68.55.ag

I. INTRODUCTION

Determination of the atomic structures formed by overlayers on surfaces is an important task for surface science. In recent years, such problems have been solved rather effectively by scanning tunneling microscopy (STM) in combinations with other structural techniques. However, there are structures that remain unsolved since their first observations in the early 1970s. An interesting example is the Ag(111) surface reacting with oxygen and chlorine. The interest in the O-Ag and Cl-Ag interactions is related to the industrial reaction of ethylene epoxidation where silver and chlorine participate as the catalyst and the promoter, respectively.[1]

The structure of the $p(4\times4)$ phase formed by oxygen on Ag(111) was decoded quite recently[2–4] but the role of this structure, as well as other oxygen structures, in the industrial process is still under debates.[5] Since the sticking probability of chlorine with silver surface is several orders of magnitude larger than the sticking probability of oxygen, even in industrial conditions the reaction of ethylene and oxygen takes place on the silver catalyst precovered with chlorine. In this connection, the atomic scale understanding of the structures formed by chlorine on Ag(111) is of profound importance. According to Campbell,[6] the promotional effect of chlorine preadsorbed on Ag(111) surface reaches its maximum at Cl coverage close to a saturation level. This high-coverage adlayer exhibits a characteristic low-energy electron diffraction (LEED) pattern described in pioneering work of Rovida *et al.*[7] as distorted 3×3. Unfortunately, even after 36 years of research no understanding whatsoever of the actual atomic structure responsible for this diffraction pattern has been achieved. In the paper, we report solving this complex structural problem from low-temperature atomic scale STM experiments and density-functional theory (DFT) calculations. We have shown that all previous models are incorrect and propose a new model which is able to explain all our experimental findings.

The structure of chlorinated silver (111) surface has been studied by LEED,[7–13] RT-STM,[14] and extended x-ray-absorption fine structure.[10,15] The room-temperature chlorine adsorption on Ag(111) gives rise to the appearance of the complex LEED pattern interpreted as distorted (3×3),[7,8] (10×10),[9,10] (17×17),[14] and double diffraction from epitaxial AgCl layer.[11,12] In fact, all the authors observed very similar LEED patterns but interpreted them in a different way. The conclusions on the surface periodicity in Ref. 14 were also made in the reciprocal space on the base of Fourier-transformed (FT) STM images due to insufficient resolution at room temperature. The aim of the present work is to properly explain this mysterious LEED pattern and determine the atomic structure responsible for it.

II. EXPERIMENTAL AND COMPUTATIONAL METHODS

All experiments were carried out in a UHV setup containing LT-STM Omicron operating at 5–77 K and LEED optics. The silver (111) sample was prepared by repetitive circles of Ar^+ bombardment (1 keV) and annealing up to 800 K. Chlorine introduction on Ag(111) was done at room temperature using a fine leak piezo-valve. All DFT calculations were carried out using the Vienna *ab initio* simulation package[16–19] employing the projector-augmented wave method[20] and Perdew, Burke, and Ernzerhof functional.[21] The plane-wave cutoff energy of 425 eV was applied. The silver substrate was modeled by a five-layer slab. During structure optimizations the top three layers of Ag atoms as well as the chlorine overlayer atoms were allowed to relax while the bottom two layers of Ag were held fixed. A vacuum layer with a thickness of 20 Å was inserted between two neighboring slabs. The integration of Brillouin zone was done using Monkhorst-Pack[22] k-point mesh $(24\times24\times1)$ per (1×1) of Ag(111). STM images were simulated from the DFT results using the simple Tersoff-Hamann approximation[23] considering states between E_F and $E_F-0.8$ eV. The simulation of the

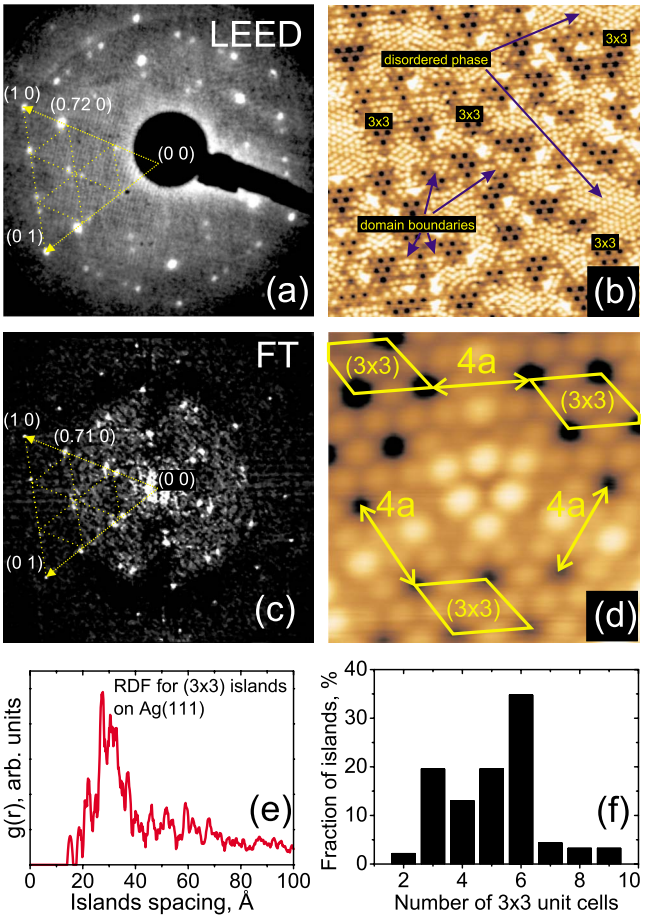

FIG. 1. (Color online) (a) LEED pattern (E_0=76 eV and 300 K) obtained for chlorine on Ag(111) at coverage close to the saturation; (b) An atomic-resolution STM image (200×200 Å^2, U_s=−1 V, I_t=1.6 nA, and 5 K) recorded at the same coverage as diffraction pattern from (a); (c) Fourier transformation of the STM image from (b); (d) fragment of the STM image showing coexistence of the antiphase (3×3) domains. The positions of the (3×3) spots in the reciprocal space in (a) and (c) correspond to knots of the grid shown by dashed lines. (e) Radial distribution function for two-dimensional array of the (3×3) islands calculated from the STM images; (f) island size distribution shown as a function of the number of the (3×3) cells in the island.

STM images has been performed for two different tip/sample distances: 2–3 Å and 3–4 Å accounting for the different experimental backloop stabilization parameters (large current/small voltage, i.e., small distance or low current/large voltage, i.e., large distance).

III. RESULTS AND DISCUSSION

Figure 1(a) shows a LEED pattern after room-temperature chlorination of the Ag(111) surface. The LEED pattern exhibits numerous spots, with bright fractional-order beams appearing at 0.72 reciprocal-lattice units between the integral order beams in good correspondence with early observations.[7–13] The cooling of the sample to 100 K did not produce any changes in the LEED pattern. The LT-STM image shows an array of triangle-shaped islands of 15–30 Å in

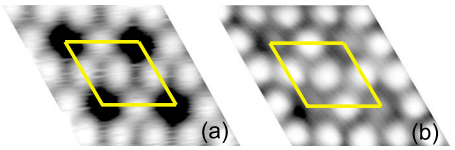

FIG. 2. (Color online) The fragments of the experimental STM images of the 3×3 island acquired at 5 K with different tunnel conditions. (a) U_s=−773 mV, I_t=0.2 nA; (b) U_s=50 mV, I_t=2.0 nA.

size on the surface, surrounded by a slightly disordered structure with atoms approximately arranged in a $(\sqrt{3}\times\sqrt{3})R30°$ lattice, as shown in Fig. 1(b). STM images recorded at 77 K have shown the same kind of islands. FT of the STM image shown in Fig. 1(c) appears to be very similar to the LEED pattern. The contribution of the disordered phase to the diffraction and FT patterns is in the increase of diffuse background.

The local structure of each island is well described by a (3×3) lattice with a unit mesh of 8.67 Å×8.67 Å [see Fig. 1(d)]. The neighboring (3×3) islands appear to be out of phase with each other as follows from Fig. 1(d). Therefore, the array of islands can be considered as a system of (3×3) antiphase domains. Note that the total number of the nonequivalent (3×3) domains on the (111) surface is equal to nine. It is well known that if antiphase domains are formed, the overlayer spots in the diffraction pattern will be split.[24–26] Indeed, the spots in Fig. 1(a) form groups around the (3×3) spots positions, i.e., the diffraction pattern can be classified as "split" (3×3). The splitting observed in LEED and FT does not correspond to formation of ordered array of the (3×3) islands. According to McKee *et al.*,[25] the splitting arises as result of the interference between beams diffracting from antiphase domains. Houston and Park[27] have shown that "sharp" splitting in diffraction pattern is produced even by the system with wide distribution of antiphase domain sizes. The amount of splitting in this case is determined by the average domain size. McKee *et al.*[25] considered the effect of separation between domains in addition to the basic antiphase interference. According to the authors, the splitting of main half-order spots remains. It depends on the domain size and the separation between domains. In our case, the distributions of the size of the (3×3) islands (10–20 Å) and the distances between them (20–40 Å) are rather sharp [see Figs. 1(e) and 1(f)] that, likely, makes possible observation of the well-defined spots both in LEED and FT.

We see that chlorine structure in average is incommensurate with the substrate. Now it is clear that in all early works authors tried to describe this complicated incommensurate structure by a single domain high-order commensurate structure, which obviously resulted in discrepancies of the data interpretation.

Now we turn to the details of atomic structure of the (3×3) phase. Figure 2(a) demonstrates a magnified fragment of the STM image of the (3×3) structure. The STM image in Fig. 2(a) shows atomic rings surrounding dark depressions. Each protrusion in Fig. 2(a) is assigned to one chlorine atom. Such interpretation is used in all works on the adsorption of halogens on fcc metals (see, for example, Refs. 28

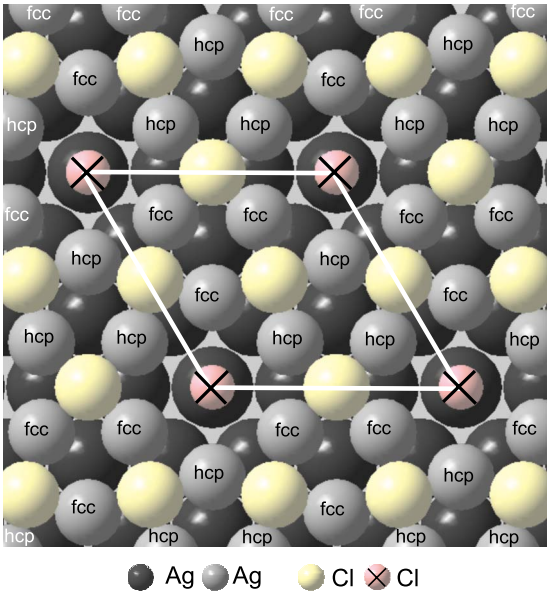

FIG. 3. (Color online) Structural model of the (3×3) reconstruction. Within (3×3) unit-cell six Ag atoms in top layer are arranged in two triangles with atoms occupying fcc and hcp sites, respectively. Chlorine atoms may be placed between four Ag atoms and on top of the silver atom in the hole.

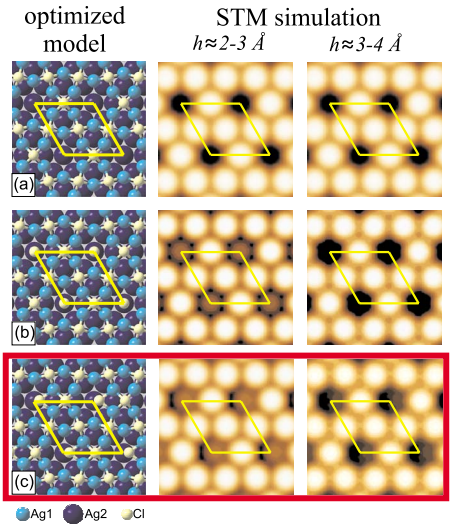

FIG. 4. (Color online) Structural models and Tersoff-Hamann simulated STM images for the (3×3) phase calculated for two different tip heights: 2–3 Å and 3–4 Å. (a) The model without atoms in the holes (coverage 0.33 ML); (b) the model with one Cl atom per hole placed in symmetrical position (coverage 0.44 ML); and (c) the equilibrium structure with one Cl atom per hole shifted off-center by 0.7 Å in the direction of the close-packed atomic rows of Ag(111) (coverage 0.44 ML).

and 29). We would also like to emphasize that at all tunneling voltages we have ever used on Ag(111) (−2 V)–(+2 V), individual chlorine atoms observed at submonolayer coverages (0.01–0.3 ML) are also visualized as protrusions. In shown below DFT simulation results for the 3×3 phase, protrusions in STM images are always associated with chlorine atoms.

The coverage estimated from the visible structure (bright atoms) is equal to 0.33 ML. However, the low-temperature LEED measurements by Shard *et al.*[10] and our recent data[30] indicated that at 0.33 ML a simple $(\sqrt{3}\times\sqrt{3})R30°$ commensurate lattice is formed while a pattern similar to that shown in Fig. 1(a) appears at higher coverage. In this connection it is reasonable to assume that centers of the rings are also occupied by chlorine atoms. To verify this idea, we acquired STM images at different tunnel currents and different bias voltages. We have established that an increase in the tunnel current to the value >2 nA with a bias voltage <100 meV leads to the appearance of small protrusions inside the holes as shown in Fig. 2(b). Assuming these protrusions are indeed additional chlorine atoms, the coverage of 0.44 ML can be estimated accordingly to the findings of Refs. 10 and 30. Interestingly, that atoms in each hole may occupy different off-center positions in correspondence with the sixfold symmetry of the ring [see Fig. 2(b)].

It is noteworthy that all bright atoms belonging to the (3×3) domains appear to be situated lower than atoms from the surrounding disordered $(\sqrt{3}\times\sqrt{3})R30°$ layer by a value of 0.5 Å irrespective to the bias voltage. The atomic modulation inside (3×3) islands also equals to 0.5 Å. All these observations indicate that the formation of the (3×3) phase is related to a reconstruction of the silver layer. Additional support to this statement is the observation of bright objects near the edges of (3×3) islands [see Fig. 1(b)]. These objects can be assigned to the excess of silver atoms extracted from the substrate.

To create an appropriate model of the (3×3) phase, we used ideas of the Ag(111)-$p(4\times4)$-O reconstruction suggested in Refs. 3 and 4. Using the same approach, six Ag atoms were left in the topmost substrate layer within the (3×3) unit cell. Three of them keep their original fcc positions and another three were moved to the hcp ones. As a result, the nearly fourfold hollow adsorption sites for chlorine atoms were created (see Fig. 3). The additional chlorine atoms can be placed in the corners of the unit cell. This model was used as a starting point of the density-functional theory calculations.

Figure 4 shows results of the optimization of atomic coordinates and corresponding simulated STM images. First, we have tested our model derived from Fig. 3 without occupancy of the corner holes by chlorine atoms. The simulated STM image in Fig. 4(a) well reproduces the experimental data with the exception of the presence of the feature in the center of the atomic rings. No protrusions appear in the hole at any parameters of the STM image simulation. In other words, the protrusion cannot be reproduced without placing an additional atom in the hole. For data shown in Fig. 4(b) the starting model included chlorine atoms in the corner holes. Our calculations demonstrate that at large tip/sample distance no bright features appear in the hole, whereas at small distance they become visible in the simulated STM images.

In the case of Fig. 4(b) the chlorine atom in the corner hole is situated on top of the silver atom from the second layer. We believed that such position does not correspond to the equilibrium. To find a new minimum, in the starting model the position of the chlorine atom was shifted by 0.1 Å

TABLE I. Calculated adsorption energies for different chlorine structures on Ag(111).

Structure	Θ (ML)	E_{ads} (eV/atom)
$(\sqrt{3}\times\sqrt{3})R30°$ (fcc)	0.33	−1.543
(3×3) Fig. 4(a)	0.33	−1.320
(3×3) Fig. 4(b)	0.44	−1.342
(3×3) Fig. 4(c)	0.44	−1.360

from the center of the ring. The result of the optimization is presented in Fig. 4(c). For chlorine atom in the hole it appears energetically more favorable to be shifted by 0.7 Å from the center of the ring in the direction of the close-packed atomic rows of Ag(111). As a result of this displacement, chlorine atom occupies position equally spaced by ≈2.7 Å from two silver atoms of the reconstructed layer and one silver atom in the hole [see Fig. 4(c)], i.e., in fact, chlorine shifts into a threefold coordination site. If remember that

TABLE II. Atomic positions of the Ag(111)-(3×3)-Cl reconstruction listed for chlorine and three upper silver layers.

Atom label	x_{DFT} (Å)	y_{DFT} (Å)	z_{DFT} (Å)
Cl	0.725	0.072	10.027
Cl	4.587	0.013	11.031
Cl	2.232	3.916	11.008
Cl	−2.192	3.812	11.006
Ag1	1.526	6.014	9.497
Ag1	−1.592	6.051	9.529
Ag1	4.420	4.332	9.515
Ag1	−0.006	3.328	9.509
Ag1	5.963	1.672	9.505
Ag1	2.856	1.659	9.533
Ag2	2.942	5.110	7.188
Ag2	−0.022	5.118	7.199
Ag2	5.890	5.103	7.172
Ag2	4.413	2.561	7.197
Ag2	1.470	2.573	7.164
Ag2	7.366	2.563	7.182
Ag2	5.890	0.009	7.184
Ag2	2.962	0.010	7.149
Ag2	−0.030	0.002	7.350
Ag3	2.958	6.824	4.826
Ag3	−0.003	6.812	4.778
Ag3	−2.974	6.827	4.821
Ag3	4.417	4.261	4.791
Ag3	1.464	4.269	4.782
Ag3	−1.484	4.261	4.781
Ag3	5.893	1.707	4.792
Ag3	2.944	1.711	4.791
Ag3	−0.008	1.687	4.822

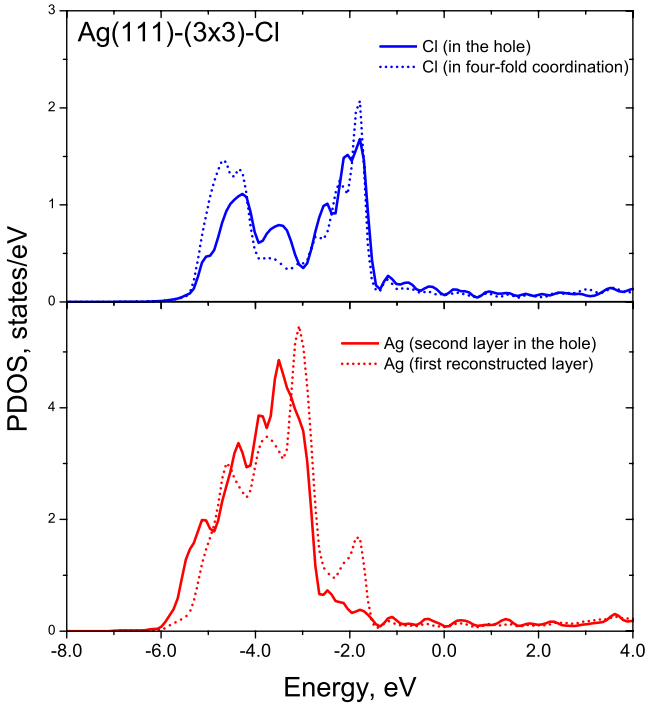

FIG. 5. (Color online) Density of states projected on chlorine and silver atoms calculated for Ag(111)-(3×3)-Cl structure. The energies are shown with respect to Fermi level.

at 0.33 ML chlorine atoms adsorbs on Ag(111) in fcc threefold hollow sites with the distance to the nearest silver atoms about 2.62–2.66 Å,[31,32] the trend to have threefold coordination is not surprising. Adsorption energies calculated for the considered above (3×3) models are listed in Table I in comparison with adsorption energy for the simple $(\sqrt{3}\times\sqrt{3})R30°$ chlorine overlayer. The energy gain of the off-center position in Fig. 4(c) compared to the symmetrical position [Fig. 4(b)] is 18 meV per atom (see Table I). The simulated STM images also demonstrate the off-center shift of the protrusion inside the atomic rings more pronounced at low tip height in good agreement with experimental STM observations [Fig. 2(b)]. Note that due to the symmetry of the system, the displacements along the six directions are equiprobable. Atomic coordinates of chlorine and three upper silver layers corresponding to the final model from Fig. 4(c) are listed in Table II.

To complete the analysis, we tried to place silver atoms in the corner holes. Similar to the case of chlorine, the simulated STM images (not shown here) demonstrate the bright feature in the center of a hole, more pronounced at low tip heights. However, we failed to get the off-center configuration of the silver atom. The DFT calculations show that the minimum of energy corresponds to the symmetrical position. This result is not in line with experimental STM observations. Moreover this model would be in disagreement with the overall Cl coverage.

Looking for the appropriate structural model of the (3×3) phase, a number of other initial structures have also been tested with DFT. The structures optimization performed for the simple (3×3) overlayer and for the corrosion layer model by Rovida and Pratesi[8] destroyed the starting models

and produced simulated STM images different from those observed in the real experiments.

Our experimental and theoretical data (see Fig. 4 and Table I) are to some extent in line with the general trend derived in the theoretical study of Cl/Ag(111) system by Gava *et al.*[33] The authors found that at coverages exceeding 0.33 ML the magnitude of adsorption energy decreased. Moreover, at critical coverage of 0.5 ML the mixed on-surface and substitutional adsorption structures becomes competitive with the simple on-surface adsorption. In these terms, the (3×3) structure corresponding to coverage of 0.44 ML can be considered as the initial stage of the mixed layer formation since Cl atoms in the hole are only 0.5 Å higher than silver atoms from the upper silver plane.

For the final (3×3) model we also calculated PDOS curves for chlorine and silver states (see Fig. 5). The clearly seen mixing of chlorine and silver states both in occupied and unoccupied part indicates the covalent bonding. Note that similar PDOS curves were reported in Ref. 33 for simple chlorine overlayer.

IV. CONCLUSIONS

In conclusion, we have established that at chlorine overlayer close to the saturation the Ag(111) surface reconstructs forming the (3×3) unit cell. Using DFT calculations, we constructed an atomic scale model of chlorinated silver (111) surface in an excellent agreement with experiment. It would be desirable to verify our model by either SXRD or dynamical LEED techniques, as was done in the case of Ag(111)-$p(4\times4)$-O,[4,34] but diffraction methods hardly make sense because of the presence of small antiphase domains of the (3×3) phase. The reconstruction Ag(111)-(3×3)-Cl decoded in the present work appears to be similar to the reconstruction Ag(111)-$p(4\times4)$-O.[3,4] Chlorine and oxygen do occupy the similar adsorption sites. This information may be important for the understanding of the chlorine role in the increase in the selectivity of ethylene epoxidation.

ACKNOWLEDGMENTS

This work was supported in part by grants of the Russian Foundation for Basic Research under Grant No. 08-02-01456-a, by Contracts No. P2452 and No. P2293 with Russian Federal Agency for Education, and by French-Russian ARCUS program. We thank Chair of Informatics, Moscow Institute of Physics and Technology, for making their MIPT-60 high performance computing system available for this work.

*andrush@kapella.gpi.ru

[1] J. G. Serafin, A. C. Liu, and S. R. Seyedmonir, J. Mol. Catal. A: Chem. **131**, 157 (1998).
[2] C. I. Carlisle, D. A. King, M. L. Bocquet, J. Cerdá, and P. Sautet, Phys. Rev. Lett. **84**, 3899 (2000).
[3] J. Schnadt, A. Michaelides, J. Knudsen, R. T. Vang, K. Reuter, E. Lægsgaard, M. Scheffler, and F. Besenbacher, Phys. Rev. Lett. **96**, 146101 (2006).
[4] M. Schmid *et al.*, Phys. Rev. Lett. **96**, 146102 (2006).
[5] R. Reichelt, S. Günther, V. Rößler, J. Wintterlin, B. Kubias, B. Jakobi, and R. Schlögl, Phys. Chem. Chem. Phys. **9**, 3590 (2007).
[6] C. T. Campbell, J. Catal. **99**, 28 (1986).
[7] G. Rovida, F. Pratesi, M. Maglietta, and E. Ferroni, Jpn. J. Appl. Phys., Suppl. **2**, 117 (1974).
[8] G. Rovida and F. Pratesi, Surf. Sci. **51**, 270 (1975).
[9] P. J. Goddard and R. M. Lambert, Surf. Sci. **67**, 180 (1977).
[10] A. G. Shard and V. R. Dhanak, J. Phys. Chem. B **104**, 2743 (2000).
[11] Y. Y. Tu and J. M. Blakely, J. Vac. Sci. Technol. **15**, 563 (1978).
[12] M. Bowker and K. C. Waugh, Surf. Sci. **134**, 639 (1983).
[13] K. Wu, D. Wang, J. Deng, X. Wei, Y. Cao, M. Zei, R. Zhai, and X. Guo, Surf. Sci. **264**, 249 (1992).
[14] B. V. Andryushechkin, K. N. Eltsov, V. M. Shevlyuga, and V. Y. Yurov, Surf. Sci. **407**, L633 (1998).
[15] G. M. Lamble, R. S. Brooks, S. Ferrer, D. A. King, and D. Norman, Phys. Rev. B **34**, 2975 (1986).
[16] G. Kresse and J. Hafner, Phys. Rev. B **47**, 558 (1993).
[17] G. Kresse and J. Hafner, Phys. Rev. B **49**, 14251 (1994).
[18] G. Kresse and J. Furthmuller, Comput. Mater. Sci. **6**, 15 (1996).
[19] G. Kresse and J. Furthmuller, Phys. Rev. B **54**, 11169 (1996).
[20] G. Kresse and D. Joubert, Phys. Rev. B **59**, 1758 (1999).
[21] J. P. Perdew, K. Burke, and M. Ernzerhof, Phys. Rev. Lett. **77**, 3865 (1996).
[22] H. J. Monkhorst and J. D. Pack, Phys. Rev. B **13**, 5188 (1976).
[23] J. Tersoff and D. R. Hamann, Phys. Rev. B **31**, 805 (1985).
[24] L. J. Clarke, *Surface Crystallography: An Introduction to Low Energy Electron Diffraction* (Wiley, New York, 1985).
[25] C. S. McKee, D. L. Perry, and M. W. Roberts, Surf. Sci. **39**, 176 (1973).
[26] C. S. McKee, M. W. Roberts, and M. L. Williams, Adv. Colloid Interface Sci. **8**, 29 (1977).
[27] J. E. Houston and R. L. Park, Surf. Sci. **21**, 209 (1970).
[28] B. V. Andryushechkin, K. N. Eltsov, and V. M. Shevlyuga, Surf. Sci. **470**, L63 (2000).
[29] W. Gao, T. A. Baker, L. Zhou, D. S. Pinnaduwage, E. Kaxiras, and C. M. Friend, J. Am. Chem. Soc. **130**, 3560 (2008).
[30] Our recent LT-STM and LEED data supported by DFT calculations evidently shown that at 0.33 ML for $T<150$ K chlorine forms a simple $(\sqrt{3}\times\sqrt{3})R30°$ well-ordered structure with one atom per unit mesh. The complex pattern from Fig. 1(a) appeared at higher coverages irrespective to the temperature of the sample.
[31] Our unpublished DFT results.
[32] N. H. de Leeuw *et al.*, Phys. Rev. B **69**, 045419 (2004).
[33] P. Gava, A. Kokalj, S. de Gironcoli, and S. Baroni, Phys. Rev. B **78**, 165419 (2008).
[34] R. Reichelt, S. Gunther, J. Wintterlin, W. Moritz, L. Aballeb, and T. O. Mentes, J. Chem. Phys. **127**, 134706 (2007).